Microwave Simulations of Precipitation Distribution with Two Radiative Transfer Models①

Liu Jinli (刘锦丽) and *Lin Longfu* (林龙福)
Institute of Atmospheric Physics, Chinese Acedemy of Sciences, Beijing 100029
Received November 10, 1993; revised April 12, 1994

ABSTRACT

Two microwave radiative transfer models of precipitating cloud are used to simulate the microwave upwelling radiances emerging from precipitating clouds. Comparison of the simulation results shows that significant difference of microwave upwelling radiances exists between these two radiative transfer models. Analysis of these differences in different cloud and precipitation conditions shows that it is complicated but has certain trend for different microwave frequencies. The results may be useful to quantitative rainfall rate retrieval of real precipitating clouds.

Key words: Radiative transfer models, Precipitation, Brightness temperature

I. INTRODUCTION

Global monitoring of precipitation is one of the challenging subjects in climate and hydrological research. Satellite remote sensing with microwave radiometers is the main method to measure global precipitation distribution. Although satellite microwave remote sensing has great potential capability in global precipitation measurements, there are some difficulties that should be considered:

a) The complexity of the vertical structures of clouds, including the water content, particle phase and size distribution in different layers. It will result in multiple relationship between the observed brightness temperature T_b and the ground rainfall rate R.

b) The inhomogeneity of horizontal finite precipitating clouds. Since the instantaneous field of view of the microwave radiometer is usually larger than single precipitating cloud cell, it may cause more complex $T_b - R$ relationship.

c) The uncertainties of surface temparature T_s and surface emissivities which may result in the difficulty of subtracting the contribution of surface emission to observed T_b.

In order to retrieve the rainfall rate with space-borne microwave radiometers, we need to find an appropriate radiative transfer model to calculate the brightness temparature and establish reliable $T_b - R$ relationship.

So far, in establishing the quantitative relationship of $T_b - R$, many investigators used the radiative transfer model with assumption of plane-parallel cloud structure (hereafter called P-P model). In fact, P-P model assumes inherently that the cloud is horizontally infinite, which inevitably overestimates the horizontal interaction of neighbouring environment in comparison with the isolated cloud cells. On the other hand, the model is unable to depict the extreme variability of precipitation which comes from horizontally finite clouds. Recently radiative transfer models describing the horizontally finite clouds are investigated by several

①This work is supported by the National Natural Science Foundation of China.

scientists, the representative work is the 3–D multi–layer model with symmetric lateral boundary conditions developed by Kummerow and Weinman (1988). Field observations show that the convective cloud is usually organized as cloud bands or clusters, it indicates that radiative interaction exists between the neighbouring clouds. For finding more suitable microwave radiative transfer models to establish better relationships between measured brightness temperatures and geophysical Table 1 parameters, especially for convective cloud bands or clusters, we developed a 3–D radiative transfer model with non–symmetric lateral boundary conditions (hereafter called it 3–D model) (Lin et al., 1994). Although in principle a 3–D model is better than a P–P model, its complexity of calculation limits its practical use. In contrary, a P–P model is relatively simple and computationally fast. Therefore, systematic comparison of the results obtained by the two models would be useful to find a feasible way of retrieving rainfall rate by a P–P model but with certain correction. As the first step of this kind comparison, we use a P–P model and a 3–D radiative transfer model with non–symmetric lateral boundary conditions to do the comparative study.

II. RADIATIVE TRANSFER MODELS

The 3–D radiative transfer model with non–symmetric lateral boundary conditions for precipitating clouds has been described in our another paper (Lin et al., 1994). Readers interested in details of the model calculation may get detailed solution and computation procedures from that paper. In principle, that 3–D model solution is obtained as follows: the 3–D equations for a precipitating cloud with vertically multi–layered hydrometeor components (ice particulates, liqiud cloud droplets and rain drops of different proportions) and horizontally finite size and homogeneous structure are solved analytically in Eddington's approximation. The lateral condition, i.e. the interaction of this model cloud with neighbouring clouds or clear atmosphere, is separated into symmetric and anti–symmetric components, and the finite Fourier transformation is used to obtain the coefficeints of above analytical solution. This model can be easily used to deal with horizontally inhomogeneous cloud band or cluster, such as those happened in tropical cloud systems, by separating the cloud band (cluster) as several horizontally homogeneous contiguous cloud cells and treating the interaction of neighbouring clouds as "lateral condition".

The P–P model we used is based on Stamnes's (1988) radiative transfer model with a little modification. In present study, we use a 3–D model and a P–P model to simulate the upwelling microwave radiances and deduce the relationship between brightness temperature and rainfall rate at 9.38, 37 and 85.6 GHz, which are recognized as the suitable frequency channels for space–borne microwave remote sensing of precipitation. The hydrometeors are assumed to be homogeneous in each layer of the vertically structured multi–layer model. Marshall–Palmer (M–P) particle size distributions are used in both liquid and ice layers. By using Mie scattering calculation algorithm, the corresponding extinction coefficeint, single scattering albedo and asymmetric factor can be obtained for each layer. For comparison study, in the two model calculation, we choose same vertical structure and same microphysical parameters of the precipitating clouds.

III. COMPUTATIONAL RESULTS

The brightness temperatures versus different rainfall rates were calculated by using the two models for nadir viewing angle over calm ocean surface. Only the results of two cases are discussed in this paper.

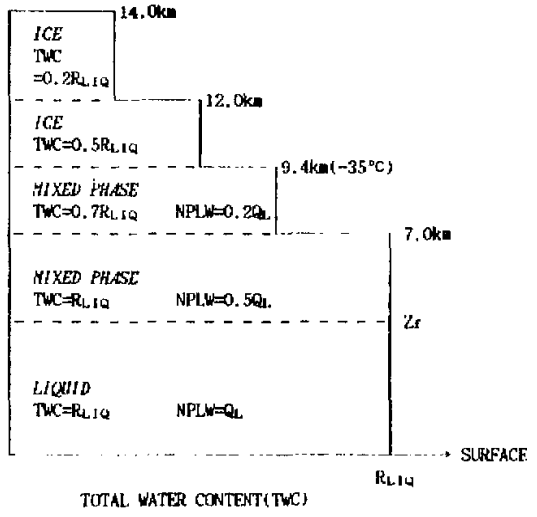

Fig. 1. The vertical structure of isolated precipitating cloud (NPLW—Non-Precipitating Liquid Water, $Q_L = 0.5$ g / m^3) (reference and modified from Wu and Weinman, 1984).

1. *Isolated Cloud Cell*

The vertical structure used in this calculation is shown in Fig. 1, which is based on the hydrometeor vertical profile deduced by Wu and Weinman (1984), and simplified in a certain degree here. In this study, the freezing level is taken as 4 km and the surface temperature is 300 K, the corresponding temperature for 7 km, 9.4 km, 12 km and 14 km height are 254 K, 238 K, 221 K and 210 K, respectively. R_{LIQ} is precipitation rate, the variation range is 2–100 mm / hr.

The upwelling radiances of precipitating cloud over calm ocean (surface albedo is 0.5) are computed with the two models at 37 GHz and 9.38 GHz channels at nadir viewing angle. In the 3–D model calculation, the lateral boundary condition is chosen as homogeneous atmosphere, and two different cloud sizes, i.e., 5 km and 10 km for 37 GHz and 5 km and 8 km for 9.38 GHz, are calculated.

The brightness temperatures versus rain rates for P–P and 3–D (cloud size $s = 5$, 8 and 10 km) model at 37 GHz and 9.38 GHz are shown in Fig. 2, Fig. 3 and Table 1. The Figures show that the global trends of two $T_b - R$ curves are different. At lower frequency, T_b increases monotonously with the increase of R (Fig. 3); At higher frequency, T_b increases with R ($< = 4$ mm / hr), and then dereases with the increase of R (Fig. 2). It has been known from the analysis of radiative transfer process that there exist two radiative processes, i.e absorption / re–emission and scattering / attenuation. At 9.38 GHz, the absorption / re–emission process plays dominant role in light and middle rain rate, and the role of scattering / attenuation gets more important when rain rate gets larger. Due to the latter (attenuation) effect is still smaller than the former (re–emission) in various rain rates ($R < = 100$ mm / hr), the compromise of these two effects would result in the increase of upwelling radiance. Therefore T_b keeps increasing with the increase of R (Fig. 3). At higher frequency, as both absorption / re–emission and scattering / attenuation processes are stronger than those at lower frequency, and the role of the upper ice layer would be

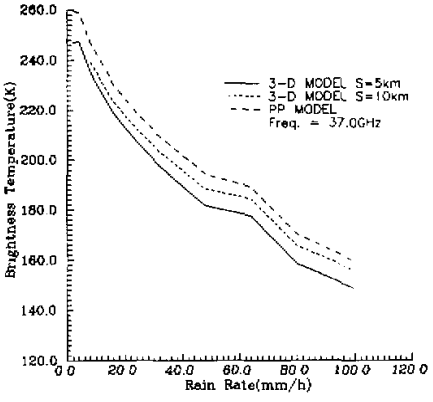

Fig. 2. Brightness temperatures versus rainfall rates for P–P and 3–D model at 37 GHz.

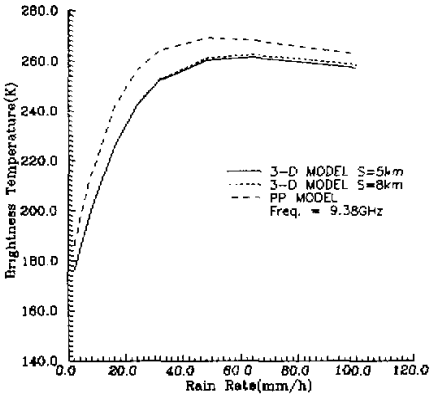

Fig. 3. Brightness temperatures versus rainfall rates for P–P and 3–D model at 9.38 GHz.

predominated, which results in reducing the upwelling radiance through scattering/attenuation process, therefore T_b increasing with R for light rainfall ($R <= 4$ mm/hr) more sharply and then decreases with the increase of R at 37 GHz (Fig. 2).

Table 1. Comparison of T_b Modeling Results Computed by 3–D and P–P Model

RR (mm/h)		2	4	8	16	24	32	48	64	80	100
Freq.	S										
9.38 (GHz)	5	176.58	184.71	200.23	225.61	242.35	252.25	260.36	261.46	259.74	257.15
	8	176.58	184.71	200.26	225.77	242.69	252.81	261.27	262.57	260.96	258.41
	∞	186.40	196.60	214.70	241.40	256.70	264.50	269.20	268.30	265.80	262.70
37.0 (GHz)	5	246.95	247.37	235.35	219.04	207.43	197.61	181.55	177.69	158.57	148.85
	10	–	–	239.20	223.43	212.49	203.38	188.37	184.47	165.74	155.53
	∞	259.60	258.80	246.90	230.40	218.90	209.60	194.20	189.20	170.40	159.30

Note: $S = 5$: Cloud Size Parameter = 5 km and T_b Computed by 3–D Model.
$S = \infty$: T_b Computed by Plane Parallel Model.

By comparing the results of the two models one can find from Fig. 2 and Table 1 that the T_b calculated by P–P model is generally higher than by 3–D model for the same rainfall rate. The range of T_b difference (ΔT_b) depends on the horizontal size of the cloud. ΔT_b increases with the decrease of the cloud size. For $s = 5$ km, ΔT_b ranges from 10.75 to 12.65 K. For $s = 10$ km, it ranges from 3.73 to 7.7 K. Similar results have been obtained for 9.38 GHz, which are shown in Fig. 3. At this frequency channel, ΔT_b ranges from 5.26 to 15.79 K for $s = 5$ km, and lower values for $s = 8$ km. These numerical results can be physically interpreted as follows. T_b calculated by P–P model is equivalent to the result of 3–D model for $s = \infty$. At relatively lower frequency channels as present situation, T_b is contributed from whole cloud column and surface emission. Interaction between neighbouring cloud cells (for $s = \infty$) will contribute more microwave flux to the lower part of the cloud column and cause more upwelling microwave radiances than isolated cloud cell. These results indicate that

if we use P–P model to estimate the upwelling radiances of an isolated (horizontally finite) cloud, the value of T_b will be over–estimated. The difference of T_b will reach to about 10 K. It is expected that in present situation the correction of P–P model calculation could be made by prior systematic comparison of numerical simulation of these two models.

2. *Cloud Band*

Owing to only a few field measurement data of cloud band have been published, in our numerical study, the cloud structure is based on a numerical modeling output simulated by Tao and Simpson (1989) for a squall line case. The $x-z$ vertical cross section of the microphysical parameters of the squall line is shown in Fig. 4. The x axis is perpendicular to the direction of squall line.

In Fig. 4, LW, CW and TIC represent Liquid Water content, Cloud Water content and Total Ice content, respectively. For doing numerical simulation, the cross–section is separated into 16 cloud profiles and the cloud size is 3 km. The microphysical parameters of each layer of the 5–layer model are obtained by averaging hydrometeor content in each layer. The comparative results of the 3–D model and P–P model at 37 GHz and 85.6 GHz are given in Fig. 5 and Table 2 and 3.

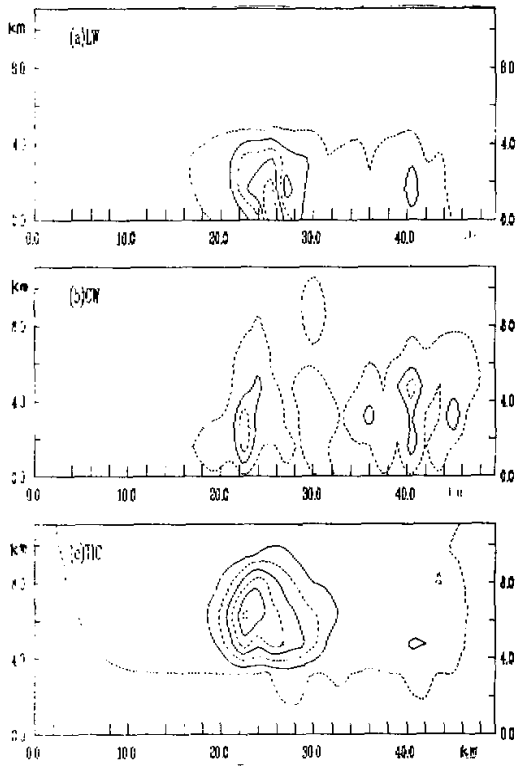

Fig. 4. The x–z vertical cross section of physical parameters at $y = 42$ km. (a) precipitating rain (1 g / m^3 interval), (b) cloud water content (0.4 g / m^3 interval), (c) total ice content (1 g / m^3 interval).

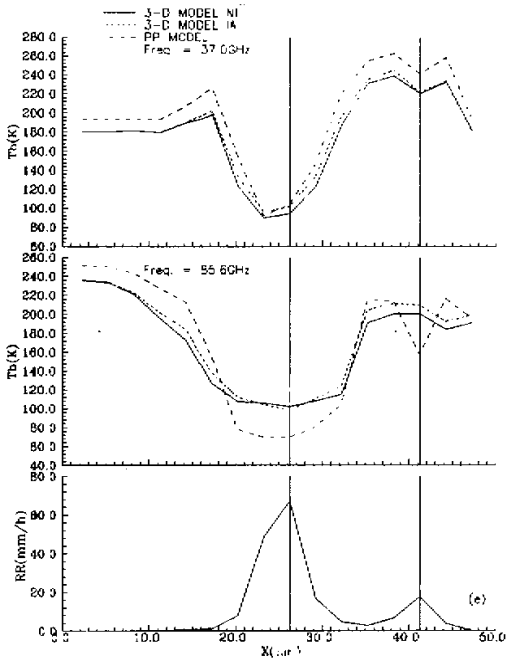

Fig. 5. T_b along x direction for P–P and 3–D model at different frequencies. (a) 37 GHz, (b) 85.6 GHz, and (c) rainfall rate distribution.

Fig. 5 (a) and (b) are the distributions of simulated T_b along x direction of the cross–section at 37.0 GHz and 85.6 GHz, respectively. *IA* and *NI* refer to the conditions with and without the interaction between neighbouring cloud in 3–D model calculation, respectively. Fig. 5(c) is the distribution of rainfall rate along the same direction.

From Fig. 5 and Fig. 4, it can be seen that at 37 GHz the brightness temperature T_b calculated by 3–D model in non–precipitating areas (at $x = 0 - 15$ km, with only thin ice cloud) is about 180 K, which is approximate to the typical value over ocean in clear sky. From $x = 15 - 18$ km, T_b increases with the light rain. It is obvious that the emission of liquid hydrometeors in the lower part of the cloud results in increase of upwelling microwave radiance. From $x = 18$ to 24 km T_b drops sharply to its lowest value 96.11 K which corresponding to the area of upper part intense ice water and lower part intense rainfall. It shows that in this situation the scattering by ice hydrometeors has dominant influence on T_b, which may results in the reduction of the upwelling radiance. The T_b rises again following the cloud water and ice water feature, both of them lead to radiance increase. The second minimum T_b (at $x = 42$ km) occurs with the ice water and light cloud water feature, it is corresponding to a small intense area of ice water and a decrease of cloud water content. The results at 85.6 GHz are shown in Fig. 5(b). It is found that T_b variation is similar to that at 37 GHz. It is known that higher frequency is more sensitive to ice water structure located on the upper part of precipitating cloud, and the lower frequency is more sensitive to cloud water and rain rate located on the lower part of the cloud. Comparing Fig. 5(a) and (b), for $x < 18$ km, T_b has a light increase due to light cloud and rain features at 37 GHz, but T_b decreases due to light ice feature at 85.6 GHz in the same range. The differences of T_b between two models are more

Table 2. T_b Modeling Results for One Cross-Section of a Squall Line at 37.0 GHz and Nadir Viewing Angle over Calm Ocean Surface

Cloud profile Number	1	2	3	4	5	6	7	8
Brightness Temperatures (*NI*) * (K)	180.43	180.39	181.23	179.50	189.33	198.18	123.02	90.17
Brightness Temperatures (*IA*) * * (K)	180.43	180.39	181.26	179.67	190.05	202.08	133.21	96.11
$\Delta T_b = T_b(IA) - T_b(NI)$	0.00	0.00	0.03	0.17	0.72	3.90	10.19	5.94
PP Model T_b Results	193.20	193.20	193.60	193.40	207.20	226.10	154.50	92.19
Cloud profile Number	9	10	11	12	13	14	15	16
Brightness Temperatures (*NI*) * (K)	94.20	123.07	188.10	231.23	238.87	220.27	232.50	181.60
Brightness Temperatures (*IA*) * * (K)	102.00	133.80	196.94	235.61	245.08	221.93	233.82	181.60
$\Delta T_b = T_b(IA) - T_b(NI)$	7.8	10.73	8.84	4.38	6.21	1.66	1.32	0.00
PP Model T_b Results	104.20	147.50	220.50	254.80	262.90	240.90	258.60	194.60

*: (*NI*) Non-Interacting between adjacent clouds;

* *: (*IA*) Interacting between adjacent clouds.

complicated. The difference of T_b is much larger than that at 37 GHz, and varies rather complicatedly. Some of T_b are over-estimated, and some are under-estimated. The largest difference is −18.97 K (at 42 km), corresponding to moderate rain and relatively high TIC value.

Comparison of the two models shows that there are significant difference between P-P and 3-D model both at 37 and 85.6 GHz channels. At 37 GHz, generally the ΔT_b (T_b (by P-P)−T_b (by 3-D)) is positive, which means T_b obtained by P-P model is larger than T_b by 3-D model, except at $x = 24$ km where the intense ice water content makes negetive ΔT_b. The variation of ΔT_b is from −3.92 K to 24.78 K. The larger ΔT_b (>20 K) happens at $x = 18$–21 km, $x = 33$ km and $x = 45$ km, corresponding to the light cloud water and rain area and relatively weak area of ice water content. The smallest ΔT_b occurs at $x = 24$ km where exists the strongest area of ice water content and cloud water and relatively intense rain rate. The above results indicate that the errors of T_b calculated by P-P model are considerably large. It strongly depends on the vertical structure of the precipitating cloud. In light rain and cloud water as well as light ice water content the error is much larger than that in intense area of ice, cloud and rain. As in the latter situation, T_b reaches to their saturation points. At 85.6 GHz, T_b difference of the two model are more complicated and have larger values. ΔT_b is from −52.16 to +28.77 K. It strongly depends on the ice water feature as well as raindrop liquid water content. It is found that for those areas where LW and TIC are both small, ΔT_b is positive. In contrary, for those areas where LW and TIC are both intense, ΔT_b turns to big

Table 3. T_b Modeling Results for One Cross Section of a Squall Line at 85.6 GHz and Nadir Viewing Angle over Calm Ocean Surface

Cloud profile Number	1	2	3	4	5	6	7	8
Brightness Temperatures (*NI*) * (K)	235.43	233.78	221.23	195.61	172.50	127.15	107.88	106.21
Brightness Temperatures (*IA*) * * (K)	235.44	234.07	222.79	201.37	183.63	137.89	112.06	104.23
$\Delta T_b = T_b(IA) - T_b(NI)$	0.01	0.29	1.56	5.76	11.13	10.74	4.18	−1.98
PP Model T_b Results	251.30	250.10	243.40	227.00	212.40	155.20	78.100	69.290
Cloud profile Number	9	10	11	12	13	14	15	16
Brightness Temperatures (*NI*) * (K)	102.06	108.41	114.90	190.61	200.46	200.38	183.84	191.21
Brightness Temperatures (*IA*) * * (K)	98.350	110.48	124.07	204.20	211.51	209.26	192.54	199.05
$\Delta T_b = T_b(IA) - T_b(NI)$	−3.71	2.07	9.17	13.59	11.05	8.88	8.70	7.84
PP Model T_b Results	69.70	80.890	104.50	215.20	213.90	157.10	216.40	196.10

*: (*NI*) Non−Interacting between adjacent clouds;

* *: (*IA*) Interacting between adjacent clouds.

negative values, such as at $x = 21 - 30$ km and $x = 42$ km. As the intense liquid water in the lower part of the cloud attenuates the emission from surface, the intense ice water in the upper part of the cloud further strongthens the multiple scattering within the upper part (cold) of the cloud. This effect is expected to be stronger in P−P model than in 3−D model. Thus the big negative ΔT_b will be obtained.

The simulation also shows that there has difference of T_b calculated by 3−D model with (*IA*) or without (*NI*) lateral interaction. At 37 GHz, the T_b difference ($\Delta T_b = T_b(IA) - T_b(NI)$) ranges from about 0 to 10 K, the bigger difference exists at those areas of intense ice water and cloud water. At 85.6 GHz, the T_b difference ranges from −3.71 K (at $x = 27$ km) to 13.59 K (at $x = 36$ km). These results show that for the 3−D model, lateral interaction of neighbouring cloud must be taken into consideration in T_b simulation.

In summary, there is big difference between brightness temperatures simulated by P−P model and 3−D model. The values and the variations of T_b difference are strongly related to the vertical structure of liquid, non−precipitating cloud and ice water except for the frequency dependence. Generally, the absoption−emission of cloud water and light rain results in increase of the radiance, and scattering of ice water and heavy rain causes decrease of the radiance. These radiative processes coexsist in the precipitating cloud and determine the brightness temperature values. For correcting P−P model, we need simultaneous observation of T_b and vertical structure of the precipitating cloud.

IV. CONCLUSION

a) Numerical simulations of space–borne microwave radiometer observation of precipitating cloud have been made with different radiative–transfer models, i.e., plane parallel model and 3–D radiative transfer model for horizontally finite cloud (both with and without interaction of neighbouring cloud).

b) Systematic discrepancy are found for results of P–P and 3–D models. It is obvious that in almost every case the P–P model results can not agree with 3–D model results (with or without lateral interaction). For lower frequency, P–P model results are always larger than 3–D model results, and the dynamic range and the "saturation" point (after that point T_b is very insensitive to the rainfall rate) for the two models are also different. For higher frequency, the difference of T_b between P–P and 3–D models shows different trend in different rainfall rates. It is owing to that the multiple scattering of ice particles plays an important role for those frequencies.

c) The numerical simulation results reveal that for wide range precipitation remote sensing of the combination of lower and higher frequencies is very important. Because P–P model is easy to use in routine base, it is possible to obtain correction from the finite cloud results by using systematic comparison of the two models.

d) For the future work, we need to use the information from both active (radar) and passive (radiometers) remote sensors to derive quantitative structure of precipitating cloud.

We thank Dr. Wu Beiying for valuable discussion in processing P–P model.

REFERENCES

Kumerrow, C. and J. A. Weinman (1988), Determining microwave brightness temperature from precipitating horizontally finite and vertically structured clouds, *J. Geophys. Res,* **93:** 3720–3728.

Lin Longfu, Lu daren, Liu Jinli, Wu Beiying (1994), Model study of microwave radiances emerging from horizontally finite precipitating clouds with different lateral boundary conditions. (To be published by Scientia Atmospherica Sinica).

Stamnes, K., S. C. Tsay, W. Wiscombe and K. Jayaweera (1988), A numerically stable algorithm for discrete–ordinate–method radiative transfer in multiple scattering and emitting layered media, *Appl. Opt.*, (June, 1988).

Tao, W.– K. and J. Simpson (1989), Modeling study of tropical sqall–type convective line, *J. Atmos. Sci.,* **46:** 177–202.

Wu, R. and J.A. Weinman (1984), Microwave radiances from precipitating clouds containing aspherical ice, combined phase, and liquid hydrometeors, *J. Geophys. Res.,* **89:** 7170–7178.